Magnetic Domain Structure in Ultrathin Films

Gabriel Bochi,[1] H. J. Hug,[2] D. I. Paul,[1] B. Stiefel,[2] A. Moser,[2] I. Parashikov,[2] H.-J. Güntherodt,[2] and R. C. O'Handley[1]

[1]*Massachusetts Institute of Technology, Cambridge, Massachusetts 02139*

[2]*Institute for Physics, University of Basel, Basel, Switzerland*

(Received 12 May 1995)

The first magnetic force microscope (MFM) images of a series of epitaxial magnetic thin films is presented. The films studied, Ni/Cu/Si(001) capped by 2 nm of Cu, exhibit perpendicular magnetization over an exceptionally broad Ni thickness range $2 < h < 14$ nm. The Ni domain structure shows a sharp transition to a finer length scale above a finite critical thickness of order 9 nm. The average force measured by the MFM tip reflects this refinement in domain structure. Micromagnetic theory, combined with our measurements of $K^{\mathrm{eff}}(h)$, provides the first quantitative description for these general but previously unexplained phenomena.

PACS numbers: 75.50.Rr, 61.16.Ch

The study of magnetic thin films is driven by scientific curiosity and technical applications. A rich variety of magnetic behaviors is observed as a function of thickness, interface structure and chemistry, strain, and preparation conditions. Applications in information storage media and in diverse sensors of magnetic field, strain, and acceleration provide further impetus to the field. Of particular importance in many applications is maintaining a preferred direction of magnetization perpendicular to the plane of a thin film. A perpendicular orientation of $\boldsymbol{M}$ defies the magnetostatic energy which tends to keep the magnetic moments oriented in the film plane. The study of thin film systems in which perpendicular magnetization is realized, e.g., fcc Fe/Cu(001) [1], bcc Fe/Ag [2], $[\mathrm{Co/Pt}]_N$ [3], $[\mathrm{Co/Au}]_N$ [4], and Ni/Cu [5–7], remains very active. In many cases the behavior of the magnetization with field is modeled assuming the ultrathin film is comprised of a single magnetic domain. However, in some ultrathin film cases, such as Co/Cu [8] and Co/Au [9] where domains have been observed, this assumption is not correct. Further it is expected that as film thickness increases domain size should first decrease then increase [10]. Also at sufficiently large film thickness the magnetostatic energy increases to a level at which $\boldsymbol{M}$ falls into the film plane. There is as yet no clear understanding of the conditions under which domains should exist in ultrathin films or of the evolution of their domain structure with film thickness. Further the mode by which the magnetization reverts to an in-plane orientation with increasing film thickness (coherent rotation or domain wall expansion) has not been resolved.

We have made an extensive study of the magnetic domain structure in Cu/Ni/Cu/Si(001) epitaxial films using a new, sophisticated high resolution magnetic force microscope (MFM). The MFM is operated in the static, variable deflection mode which is well suited for high-speed images of large areas [11,12]. A special nonmagnetic tip, sharpened by vacuum carburization and coated with a thin e-beam deposited $\mathrm{Co_{80}Ni_{20}}$ layer [13] was scanned over the magnetic films at a height of approximately 30 nm. The samples studied are a series of molecular-beam-epitaxy-grown, epitaxial Ni/Cu/Si(001) films capped with 2 nm of Cu. The Cu buffer layer is typically 200 nm thick and the samples are 1 cm^2 in area. These films had previously been fully characterized *in situ* before capping using reflection high-energy electron diffraction (RHEED) [14] and the magneto-optic Kerr effect [5,7] and *ex situ* after capping using vibrating sample magnetometry [6] and optical interferometry (for strain measurements) [14]. The Cu/Ni/Cu/Si(001) system shows an extremely broad thickness range (2 to 14 nm) over which perpendicular magnetization is observed [6]. This allows for careful study of several important phenomena characteristic of magnetic thin films. Here we show that MFM can resolve domains in magnetic films as thin as 2 nm and report the first detailed experimental confirmation of a micromagnetic model predicting a transition to an essentially infinite domain size below a critical thickness of a magnetic film. We also show measurements and analysis of the film thickness dependence of the MFM force above magnetic films of different domain structure. Finally, the MFM images indicate that the perpendicular to in-plane transition with increasing film thickness is not achieved by coherent rotation of domain magnetization but rather by multiplication of domain walls whose magnetization lies in the film plane.

Magnetic domains were imaged in sandwiches containing from 2 to 17.5 nm of Ni (selected images are shown in Fig. 1–4). To our knowledge, MFM domain images have never been reported on such thin films of any composition and domain images taken by any technique are not available on such thin Ni films [8,9]. The MFM images confirm dramatically that the magnetization is indeed strongly held to a perpendicular direction as indicated by the magneto-optic Kerr effect loops [5,7] and vibrating-sample magnetometer measurements [6]. In these images the contrast is due to magnetization into and out of the

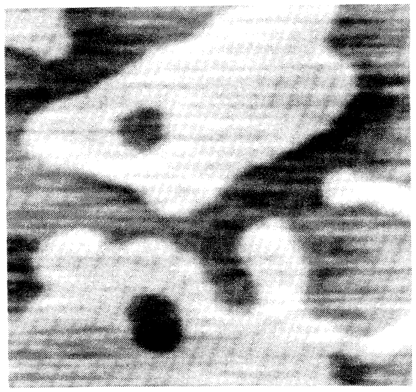

FIG. 1. Domain structure of Cu/2 nm Ni/Cu(001) over a 12 μm square.

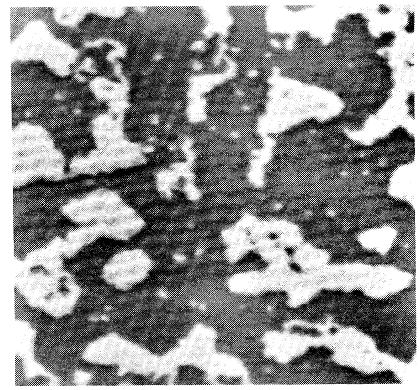

FIG. 3. Domain structure of Cu/10 nm Ni/Cu(001) over a 12 μm square.

plane of the paper; no regions of in-plane magnetization were observed other than the domain walls themselves.

It is noteworthy that the domain walls show no orientational correlation with the easy in-plane $\langle 110 \rangle$ crystallographic directions in these epitaxial Ni films. This will be the subject of a forthcoming paper. The domain walls are Bloch walls, not Néel walls, so the wall magnetization runs along the wall length with no cost in magnetostatic energy. (Néel walls are preferred only in thin films exhibiting in-plane magnetization.) Based on our magnetic anisotropy measurements [6], the wall width $\delta_{\mathrm{dw}} = \pi(A/K)^{1/2}$ should be of order 30 nm for a Ni thickness of 8.5 nm and increases for thinner or thicker films.

The domain structure is characterized by two types of behavior in different thickness ranges. At and below 8.5 nm of Ni the domain patterns are irregularly spotted (Fig. 1) and tend toward serpentine patterns at larger thickness h (Fig. 2). The length scale of this coarse structure is poorly defined, but its average decreases with increasing h. Relative to the film thickness, these patterns are essentially infinite in lateral scale (1–4 μm) and so may be characterized by a reduced domain size parameter $D/h \approx \infty$. The weak energies that govern these features are not yet well understood. Above 8.5 nm the relatively large serpentine domains begin to break down by internal fragmentation (submicron bubble domain formation) as seen in Figs. 3 and 4. It is noteworthy that the larger domain features that characterize the thinner Ni films (Figs. 1 and 2) are preserved even as the internal fragmentation of the domains progresses with increasing thickness above 10 nm (Fig. 3 and 4). This suggests that these separate-scale structures may be governed by different energies and/or kinetics. As the Ni thickness increases, magnetostatic energy is reduced by refinement of the interior bubble domain structure rather than by more complex contortions of the existing domain walls. This occurs because the magnetostatic energy well inside a domain is $(\mu_0/2)M_z^2$, while it is significantly reduced near an existing domain wall. The submicron length scale of the finer features decreases markedly with increasing Ni

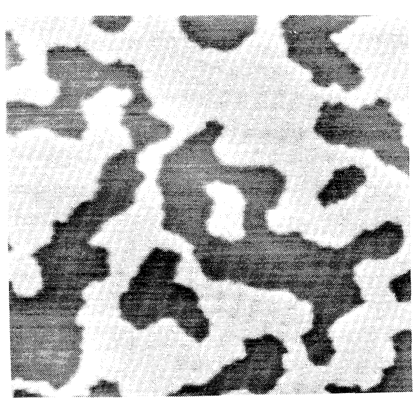

FIG. 2. Domain structure of Cu/8.5 nm Ni/Cu(001) over a 12 μm square.

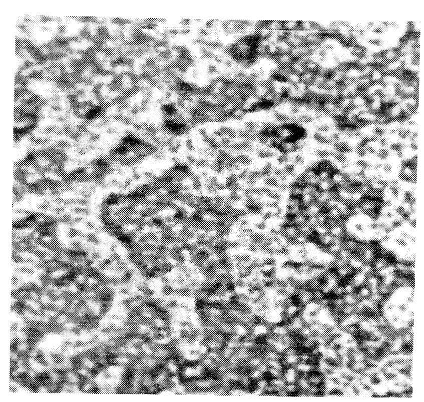

FIG. 4. Domain structure of Cu/12.5 nm Ni/Cu(001) over a 12 μm square.

thickness. We can calculate the transition to this finer domain structure and its length scale by extensions of domain theory as outlined by Kittel [15] and developed by others [10,16–18].

As shown in Ref. [10], the energy difference between stripe and checker domain patterns is small. Neglecting the finite width of the domain walls, we may use the expression for the energy per unit surface area for a stripe domain structure, i.e.,

$$u = 16M_s^2 \frac{D}{\pi^2} \sum_n^{\text{odd}} \frac{1 - \exp[-n\pi h/D]}{n^3} + \frac{h\sigma_{\text{dw}}(h)}{D}, \tag{1}$$

where we write the domain wall energy density $\sigma_{\text{dw}}(h) = 4(AK^{\text{eff}})^{1/2}$ as a function of Ni thickness because of the strong dependence of the measured effective anisotropy K^{eff} on thickness [6]. We have numerically minimized Eq. (1) with respect to the domain size, using the methods of Malek and Kambersky [16]. For the range of interest here, $h < 14$ nm, we have plotted the numerical solution in Fig. 5 using the experimentally measured [6] effective anisotropy K^{eff} in σ_{dw}, $A = 1 \times 10^{-6}$ erg/cm and $M_s \approx 435$ emu/cm^3. This magnetization density is smaller than the bulk value for Ni, 485 emu/cm^3, but is typical of that measured for our films in this thickness range. The thickness corresponding to the onset of domain fragmentation is calculated to be approximately 10 nm and the average domain spacing is calculated to decrease to about 0.2 μm for $h = 12.5$ nm. The domain images indicate that between $h_{\text{Ni}} = 8.5$ and 10 nm the fine domains first appear in our Cu/Ni/Cu sandwiches and their separation distance decreases with increasing Ni thickness in agreement with the theory.

Although the calculated value of D begins to increase rapidly near 10 nm, the energy minimum vs D, from Eq. (1), up to about 10 nm is extremely shallow, suggesting that at finite temperatures a broad range of D values would be allowed. Only above $h \approx 10$ nm does the energy minimum become well defined forcing the domain structure to take on a more periodic structure.

These results comprise the first verification in any thin film system of the effective divergence of the domain size at a finite thickness and of the transition from a well-defined periodic domain structure at large thicknesses to a much more variable one with decreasing film thickness. The theoretical fit by $D(h)$, plotted here for the first time, makes use of our own measurements of K^{eff} in Cu/Ni/Cu/Si(001) [6].

The magnitude of the average vertical MFM force difference measured from domain to domain (away from the walls), $\langle \Delta F_Z \rangle$, is shown by the solid data points in Fig. 6. The Ni thickness dependence of this force varies somewhat like the strength of the effective anisotropy per unit area [6]; i.e., the strongest force difference is detected above films having the strongest perpendicular anisotropy. The sharp drop in force above a Ni thickness

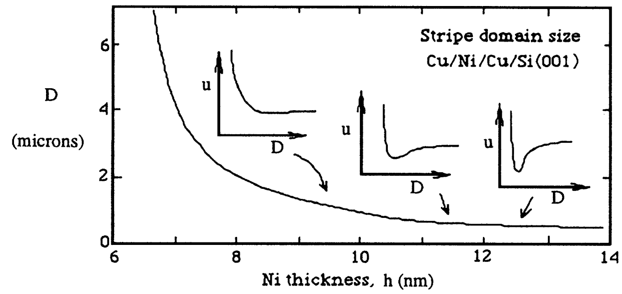

FIG. 5. Ni thickness dependence of domain size by numerical minimization of the energy u in Eq. (1) using independently measured effective anisotropy [6]. Insets show the shape of the energy minima at Ni thicknesses of 9.5, 11.5, and 12.5 nm.

of approximately 10 nm is the result of the onset of internal fragmentation of the large ($D > 1$ μm) domains into submicron bubble domains; this fragmentation strongly attenuates the average vertical fringe field measured above the film.

The force on the MFM tip comes almost entirely from the poles on the lower end of the tip because the field is essentially zero at the upper end (the tip is 0.5 μm long). Thus the vertical force on the MFM tip is the integral over the tip area of the product of the field B_z and the pole strength of the tip. The near field above a magnetic dipole $\mu_m = M_{\text{Ni}} \pi a^2 h$ is

$$B_z = \frac{\mu_0}{4\pi} \frac{2\mu_m}{(a^2 + z^2)^{3/2}}. \tag{2}$$

where a, the radius of the domain dipole, is much greater than the scanning height $z \approx 30$ nm. The field B_z is representative of the magnetization at the center of a perpendicular domain. When the domain pattern fragments into a finer pattern which we assume to be periodic of wavelength $\lambda = 2D$, the attenuation of the vertical field at sufficient height above the film can be approximated by an additional factor [19] $\exp[-kz]$, where $k = 2\pi/\lambda$. The vertical force then becomes

$$F_z \approx \mu_0 M_{\text{Ni}} M_{\text{tip}} A_{\text{tip}} \frac{h}{2a} e^{-kz}. \tag{3}$$

For $h < 10$ nm, the domain patterns are so large that $e^{-kz} \approx 1$. The positive curvature of $\langle \Delta F \rangle$ vs h observed

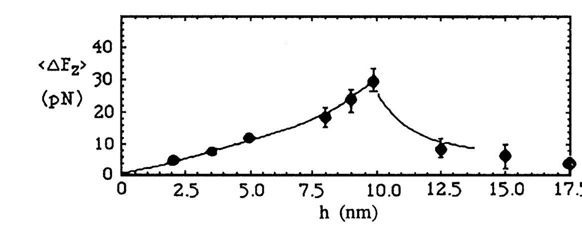

FIG. 6. Variation with Ni thickness of average difference in vertical MFM force measured between adjacent domains. Solid lines are fits to the data using Eq. (3).

in the thin Ni regime is related to the decreasing size of the coarse domain structure with increasing film thickness. Above the fragmentation limit, $h > 10$ nm, λ quickly assumes a value of order 0.4 μm as h increases (see Fig. 6), and the force is predicted to be linear in h/a with an exponential attenuation factor when the domain pattern becomes fragmented. Further the effect of the finite width of the tip, $w \approx 40$ nm, can be approximated by increasing its height above the medium in Eq. (3) to $z + w \approx 70$ nm [20]. In this large-Ni-thickness range, the solid curve in Fig. 6 is given by Eq. (3) as $\langle \Delta F \rangle \approx 30 \exp(-0.1/a)$ with a in microns, h in nanometers, and ΔF_Z in piconewtons. The theoretical fit is not extended above 14 nm because above that limit $K^{\mathrm{eff}} < 0$. This simple model represents a good first order approximation to the behavior actually observed.

Above a Ni thickness of 14 nm where magnetometry [21] indicates the easy magnetization axis is in plane, the Bloch domain walls are very broad and probably represent more than half of the film surface area. It is important to note that a net perpendicular MFM force difference is still observed in this thickness regime. This suggests that the net in-plane magnetization measured by magnetometry at 15 nm Ni may be due to the broad Bloch walls between smaller, perpendicularly magnetized regions. Magnetization measurements reveal the net in-plane moment whereas MFM detects the fringe field above the small, perpendicular regions. Thus the easy axis transition in these films appears to be a result of wall broadening rather than coherent rotation of perpendicular $\boldsymbol{M}$ into the film plane. This important issue will be addressed in future studies as improved MFM resolution is realized.

In summary, we have measured the domain size in a series of epitaxial Ni/Cu films over the Ni thickness range $2 < h < 17.5$ nm using a high resolution MFM. From 2 up to 10 nm of Ni the domains are large and of a relatively irregular size; their average size decreases with increasing Ni thickness. Between 8.5 and 10 nm of Ni internal fragmentation of the larger domains into submicron bubble domains begins. The size and spacing of these internal bubble domains decreases to approximately 0.2 μm at $h = 12.5$ nm. These finer domains are more uniform in their spacing than are the coarser domains observed below 10 nm. All of these features are well described by micromagnetic domain theory. The measured MFM force difference between adjacent domains shows a well-defined variation with Ni thickness. This variation can be reasonably well modeled by expressions for the interaction of a long, vertical dipole tip of finite width with a dipole medium having the domain size observed.

This work was supported in part by NSF Grant No. DMR 9410943 and by the Swiss National Science Foundation. We thank Manfredd Rührig and Steffen Porthun for the electron-beam fabrication of the MFM tip.

[1] D. Pescia, M. Stampanoni, G.L. Bona, A. Vaterlaus, R.F. Willis, and F. Meier, Phys. Rev. Lett. **58**, 2126 (1987); C. Liu, E.R. Moog, and S. Bader, Phys. Rev. Lett. **60**, 2422 (1988); D.P. Pappas, K.P. Kämper, and H. Hopster, Phys. Rev. Lett. **64**, 3179 (1990).
[2] M. Stampanoni, A. Vaterlaus, M. Aeschlimann, and F. Meier, Phys. Rev. Lett. **59**, 2483 (1987).
[3] B.N. Engle, C.D. England, R.A. Van Leeuwen, M.H. Wiedemann, and C.M. Falco, Phys. Rev. Lett. **67**, 1910 (1991).
[4] F.J.A. de Broeder, D. Kuiper, A.P. van de Mosselaer, and W. Hoving, Phys. Rev. Lett. **60**, 2769 (1988); C.H. Lee, H. He, F.J. Lamelas, W. Vavra, C. Uher, and R. Clark, Phys. Rev. B **42**, 1066 (1990).
[5] G. Bochi, C.A. Ballentine, H.E. Inglefield, S.S. Bogomolov, C.V. Thompson, and R.C. O'Handley, Mater. Res. Soc. Symp. Proc. **313**, 309 (1993).
[6] G. Bochi, C.A. Ballentine, H.E. Inglefield, C.V. Thompson, and R.C. O'Handley (to be published).
[7] G. Bochi, C.A. Ballentine, H.E. Inglefield, C.V. Thompson, R.C. O'Handley, H.J. Hug, B. Stiefel, A. Moser, and H.-J. Güntherodt, Phys. Rev. B (to be published).
[8] H.P. Oepen, M. Benning, H. Ibach, C.M. Schneider, and J. Kirschner, J. Magn. Magn. Mater. **86**, 137 (1990).
[9] R. Allenspach, M. Stampanoni, and A. Bischof, Phys. Rev. Lett. **65**, 3344 (1990); R. Allenspach and A. Bischof, Phys. Rev. Lett. **69**, 3385 (1992).
[10] B. Kaplan and G.A. Gehring, J. Magn. Magn. Mater. **128**, 111 (1993).
[11] A.M. Schoenberger and S. Alvarado, Z. Phys. B **80**, 373 (1990).
[12] H.J. Hug, Ph.D. thesis, Universität Basel, 1993; H.-J. Hug, A. Moser, Th. Jung, A. Wadas, I. Parashikov, and H.-J. Güntherodt, Rev. Sci. Instrum. **64**, 2925 (1993).
[13] M. Rührig, S. Poerthun, and J.C. Lodder, Rev. Sci. Instrum. **65**, 3244 (1994).
[14] H.E. Inglefield, C.A. Ballentine, G. Bochi, S.S. Bogomolov, R.C. O'Handley, and C.V. Thompson, Mater. Res. Soc. Symp. Proc. **308**, 765 (1993); H.E. Inglefield, G. Bochi, C.A. Ballentine, R.C. O'Handley, and C.V. Thompson, Mater. Res. Soc. Symp. Proc. (to be published).
[15] C. Kittel, Phys. Rev. **70**, 945 (1946).
[16] Z. Malek and V. Kambersky, Czech. J. Phys. **8**, 416 (1958).
[17] C. Kooy and U. Enz, Philips Res. Rep. **15**, 7 (1960).
[18] Y. Yafet and E.M. Gyorgy, Phys. Rev. B **38**, 9145 (1988).
[19] R.L. Wallace, Bell Syst. Tech. J. **30**, 1145 (1951).
[20] H.N. Bertram, *Theory of Magnetic Recording* (Cambridge University Press, Cambridge, England, 1994), p. 96.
[21] G. Bochi, Ph.D. thesis, Massachusetts Institute of Technology, 1995.

FIG. 1. Domain structure of Cu/2 nm Ni/Cu(001) over a 12 μm square.

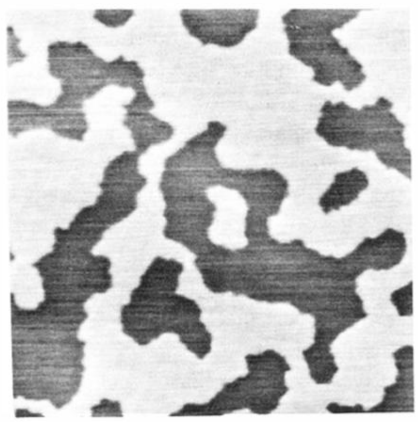

FIG. 2. Domain structure of Cu/8.5 nm Ni/Cu(001) over a 12 μm square.

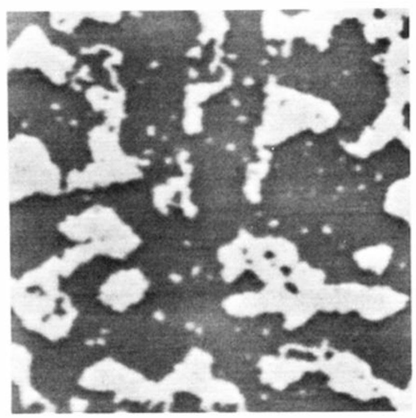

FIG. 3. Domain structure of Cu/10 nm Ni/Cu(001) over a 12 μm square.

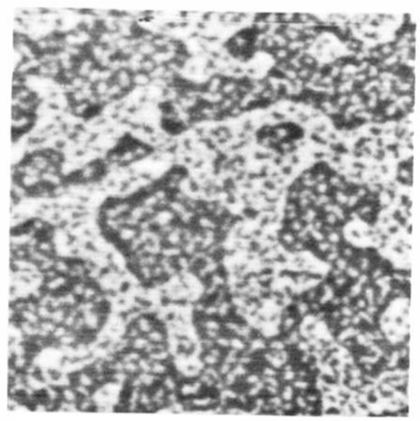

FIG. 4. Domain structure of Cu/12.5 nm Ni/Cu(001) over a 12 μm square.